International Journal of Cardiology 167 (2013) 698–703

Contents lists available at SciVerse ScienceDirect

International Journal of Cardiology

journal homepage: www.elsevier.com/locate/ijcard

Heart failure-induced skeletal myopathy in spontaneously hypertensive rats ☆

R.L. Damatto [a,b], P.F. Martinez [a,b], A.R.R. Lima [a,b], M.D.M. Cezar [a,b], D.H.S. Campos [a,b], S.A. Oliveira Junior [a,b,c], D.M. Guizoni [a,b], C. Bonomo [a,b], B.T. Nakatani [a,b], M. Dal Pai Silva [d,e], R.F. Carvalho [d,e], K. Okoshi [a,b], M.P. Okoshi [a,b,*]

[a] Department of Internal Medicine, Botucatu Medical School, Sao Paulo State University, UNESP, Brazil
[b] Departamento de Clinica Medica, Faculdade de Medicina de Botucatu, Rubiao Junior, S/N 18618 970, Botucatu, SP, Brazil
[c] Federal University of Mato Grosso do Sul, Campo Grande, Brazil
[d] Department of Morphology, Institute of Biosciences, Sao Paulo State University, UNESP, Brazil
[e] Departamento de Morfologia, Instituto de Biociencias, Rubiao Junior S/N, Botucatu, SP, Brazil

ARTICLE INFO

Article history:
Received 15 December 2011
Received in revised form 2 March 2012
Accepted 3 March 2012
Available online 30 March 2012

Keywords:
Heart failure
Skeletal myopathy
Muscle atrophy
Fibrosis
Myosin heavy chain
Spontaneously hypertensive rat

ABSTRACT

Background: Although skeletal muscle atrophy and changes in myosin heavy chain (MyHC) isoforms have often been observed during heart failure, their pathophysiological mechanisms are not completely defined. In this study we tested the hypothesis that skeletal muscle phenotype changes are related to myogenic regulatory factors and myostatin/follistatin expression in spontaneously hypertensive rats (SHR) with heart failure.
Methods: After developing tachypnea, SHR were subjected to transthoracic echocardiogram. Pathological evidence of heart failure was assessed during euthanasia. Age-matched Wistar–Kyoto (WKY) rats were used as controls. Soleus muscle morphometry was analyzed in histological sections, and MyHC isoforms evaluated by electrophoresis. Protein levels were assessed by Western blotting. Statistical analysis: Student's *t* test and Pearson correlation.
Results: All SHR presented right ventricular hypertrophy and seven had pleuropericardial effusion. Echocardiographic evaluation showed dilation in the left chambers and left ventricular hypertrophy with systolic and diastolic dysfunction in SHR. Soleus weight and fiber cross sectional areas were lower (WKY 3615±412; SHR 2035±224 μm^2; $P<0.001$), and collagen fractional volume was higher in SHR. The relative amount of type I MyHC isoform was increased in SHR. Myogenin, myostatin, and follistatin expression was lower and MRF4 levels higher in SHR. Myogenin and follistatin expression positively correlated with fiber cross sectional areas and MRF4 levels positively correlated with I MyHC isoform.
Conclusion: Reduced myogenin and follistatin expression seems to participate in muscle atrophy while increased MRF4 protein levels can modulate myosin heavy chain isoform shift in skeletal muscle of spontaneously hypertensive rats with heart failure.

1. Introduction

Heart failure is characterized by reduced exercise tolerance with early occurrence of fatigue and dyspnea. In addition to cardiac dysfunction and pulmonary abnormalities, intrinsic skeletal muscle changes can be involved in reduced physical capacity [1–4]. Several skeletal muscle abnormalities have been described in patients and animals with heart failure; these include atrophy, fibrosis, altered myosin heavy chain (MyHC) composition, and decreased oxidative capacity [1,2,5–9].

The mechanisms and intracellular signaling pathways involved in heart failure-induced skeletal muscle abnormalities are not completely understood. There is substantial evidence that myogenic regulatory factors (MRF) MyoD, myogenin, Myf5, and MRF4 act as important regulators of muscle protein expression [10–12]. MRFs are transcriptional factors that activate the expression of muscle specific genes. Myogenin is preferentially expressed in slow twitch fibers and modulates the expression of oxidative enzymes [13]. MyoD, which is preferentially expressed in fast muscle fibers, participates in muscle regeneration [11,14]. MRF4 may play a role in preserving differentiated muscle state [15]. Few studies have evaluated MRFs during heart failure. Our laboratory has observed decreased mRNA levels for MyoD and MRF4 in soleus muscle of rats with rapid onset heart failure [16] while rats with chronic heart failure presented decreased myogenin protein levels [5].

☆ Grants: Financial support was provided by CNPq (305013/2009-0 and 304998/2009-5), FAPESP (2009/54857-4, 2009/54102, and 2010/50461-6) and Fundunesp (01197/08).

* Corresponding author at: Departamento de Clinica Medica, Faculdade de Medicina de Botucatu, UNESP, Rubiao Junior, S/N 18618-970, Botucatu, SP, Brazil. Tel.: +55 14 3882 2969; fax: +55 14 3882 2238.
E-mail address: mpoliti@fmb.unesp.br (M.P. Okoshi).

0167-5273/$ – see front matter © 2012 Elsevier Ireland Ltd. All rights reserved.
doi:10.1016/j.ijcard.2012.03.063

Myostatin, a member of the transforming growth factor-beta superfamily, modulates muscle growth, acting as a negative regulator of skeletal muscle mass [17,18]. Studies on its physiological role have shown a negative correlation between myostatin gene expression and muscle mass, suggesting a potential to induce skeletal muscle atrophy [17,19,20]. Myostatin activity can be modulated by various proteins. Follistatin has emerged as a potent myostatin antagonist which acts by modifying its *in vivo* activity [21–23]. Few authors have assessed the myostatin/follistatin pathway in heart failure [6,24]. In our laboratory, rats with myocardial infarction-induced heart failure presented muscle atrophy in combination with unchanged myostatin levels and decreased follistatin protein expression [6].

One widely used experimental model for studying heart failure is the spontaneously hypertensive rat (SHR). It presents early arterial hypertension and left ventricular hypertrophy which evolves to heart failure during maturity and senescence. As cardiac failure development is slow, SHRs are considered a useful model to mimic clinical heart failure settings. In this study we characterized skeletal muscle changes of SHR with heart failure by evaluating muscle trophism, fibrosis, and myosin heavy chain isoforms. We tested the hypothesis that heart failure-induced skeletal muscle phenotype changes are related to myogenic regulatory factors and myostatin/follistatin protein expression changes.

2. Materials and methods

2.1. Experimental groups

Male spontaneously hypertensive rats (SHR) and non-hypertensive Wistar–Kyoto (WKY) rats were purchased from the Central Animal House at Botucatu Medical School, UNESP. All animals were housed in a room under temperature control at 23 °C and kept on a 12-hour light/dark cycle. Food and water were supplied *ad libitum*. All experiments and procedures were approved by the Ethics Committee of Botucatu Medical School, UNESP, Botucatu, SP, Brazil.

Systolic arterial pressure was measured by the tail-cuff method at fifteen months of age. Beginning at 18 months old, all rats were observed twice weekly to identify clinical heart failure features. Animals were studied after heart failure had been detected, which was characterized by tachypnea and labored respiration. Age matched WKY rats were studied at comparable ages. After diagnosing heart failure, rats were subjected to transthoracic echocardiography and euthanized two days after. During euthanasia, we evaluated pathological evidence of heart failure such as pleuropericardial effusion, left atrial thrombi, ascites, pulmonary congestion (lung weight-to-body weight ratio > 2 standard deviations above the mean for the WKY group) [25], and right ventricular hypertrophy (right ventricle weight-to-body weight ratio > 0.8 mg/g) [26–29].

At the time of euthanasia, the animals were weighed, anesthetized with intraperitoneal sodium pentobarbital (50 mg/kg), and decapitated. The heart was removed by thoracotomy and the atria and ventricles were separated and weighed. Both right and left soleus muscles were excised, weighed, immediately frozen in liquid nitrogen, and stored at −80 °C. Fragments of liver were weighed before and after drying sessions (65 °C for 72 h) to evaluate wet/dry weight ratio.

2.2. Echocardiographic study

Echocardiographic evaluation was performed using a commercially available echocardiograph (General Electric Medical Systems, Vivid S6, Tirat Carmel, Israel) equipped with a 5–11.5 MHz multifrequency transducer. Rats were anesthetized by intramuscular injection of a mixture of ketamine (50 mg/kg) and xylazine (0.5 mg/kg). A two-dimensional parasternal short-axis view of the left ventricle (LV) was obtained at the level of the papillary muscles. M-mode tracings were obtained from short-axis views of the LV at or just below the tip of the mitral-valve leaflets, and at the level of the aortic valve and left atrium [29,30]. M-mode images of the LV were printed on a black-and-white thermal printer (Sony UP-890MD) at a sweep speed of 100 mm/s. All LV structures were manually measured by the same observer according to the leading-edge method of the American Society of Echocardiography [31]. The measurements obtained were the mean of at least five cardiac cycles on the M-mode tracings. The following structural variables were measured: left atrium (LA) diameter, LV diastolic and systolic dimensions (LVDD and LVSD, respectively), LV diastolic posterior wall thickness (PWT), LV diastolic septal wall thickness (SWT), and aortic diameter (AO). Left ventricular function was assessed by the following parameters: heart rate (HR), endocardial fractional shortening (FS), LV ejection fraction (EF), posterior wall shortening velocity (PWSV), early-to-late diastolic mitral inflow ratio (E/A ratio), E-wave deceleration time (EDT), and isovolumetric relaxation time (IVRT).

2.3. Morphologic study

Serial transverse sections of the soleus muscles were cut at 8 μm thickness in a cryostat cooled to −20 °C and stained with hematoxylin and eosin. At least 150 cross-sectional fiber areas were measured from each soleus muscle. Other slides were stained with Sirius Red F3BA and used to quantify interstitial collagen fraction [32]. On average, 20 microscopic fields were analyzed with a 40X lens. Perivascular collagen was excluded from this analysis. Measurements were taking using a compound microscope (Leica DM LS; Nussloch, Germany) attached to a computerized imaging analysis system (Media Cybernetics, Silver Spring, MD, USA).

2.4. Myosin heavy chain (MyHC) isoforms

MyHC isoform analysis was performed in duplicate by sodium dodecyl sulphate polyacrylamide gel electrophoresis (SDS-PAGE). Frozen samples of soleus muscle (100 mg) were mechanically homogenized on ice in 0.8 mL of protein extraction solution containing 50 mM phosphate potassium buffer (pH 7.0), 0.3 M sucrose, 0.5 mM dithiotreitol (DTT), 1 mM ethylenediaminetetraacetic acid (EDTA), 0.3 mM phenylmetylsulphonyl fluoride (PMSF), 10 mM sodium fluoride and protease inhibitor cocktail (Sigma, St. Louis, MO, USA). Homogenates were centrifuged at 12,000 × *g* at 4 °C for 20 min to remove insoluble tissue. Total protein quantification was performed in supernatant aliquots by the Bradford method. Samples were then diluted to a final concentration of 1 μg of protein/μL in a solution containing 65% (vol/vol) glycerol, 2.5% (vol/vol) 2-mercaptoethanol, 1.15% (wt/vol) SDS, and 0.45% (wt/vol) Tris–HCl (pH 6.8). Small amounts of the diluted extracts (15 μL) were loaded onto a 7–10% SDS-PAGE separating gel with a 4% stacking gel, run overnight (24–30 h) at 120 V, and stained with Coomassie blue. Two MyHC isoforms, MyHC I and MyHC IIa, were identified according to the molecular mass and quantified by densitometry. Their relative amounts were expressed as the percentage of the total amount of myosin heavy chain.

2.5. Western blotting analysis

Protein levels of soleus muscle were analyzed by Western blotting according to a previously described method [33,34] with specific anti-myogenin (M-225, sc-576), anti-MyoD (M-318, sc-760), anti-MRF4 (C-19, sc-301), anti-myostatin (N-19-R sc-6885-R) or anti-follistatin (H-114 sc-30194) antibodies (Santa Cruz Biotechnology, Santa Cruz, CA, USA). Protein levels were normalized to those of GAPDH (6 C5, sc-32233, Santa Cruz Biotechnology). Muscle protein was extracted using Tris-Triton buffer (10 mM Tris pH 7.4, 100 mM NaCl, 1 mM EDTA, 1 mM EGTA, 1% Triton X-100, 10% glycerol, 0.1% SDS, 0.5% deoxycholate). Supernatant protein content was quantified by the Bradford method. Samples were separated on a polyacrylamide gel and then transferred to a nitrocellulose membrane. After blockage, membrane was incubated with the primary antibody. Membrane was washed with TBS and Tween 20 and incubated with secondary peroxidase-conjugated antibody. Super Signal® West Pico Chemiluminescent Substrate (Pierce Protein Research Products, Rockford, USA) was used to detect bound antibodies.

2.6. Statistical analysis

Data are expressed as mean ± standard deviation. Comparisons between the groups were performed by Student's-*t* test. Associations between variables were assessed with Pearson's correlation coefficient. The level of significance was set at 5%.

3. Results

3.1. Group characterization and anatomic parameters

In SHR ($n = 8$), all rats presented right ventricular hypertrophy, 7 had pleuropericadial effusion, 5 pulmonary congestion, 4 atrial thrombi, and 3 ascites. There was no clinical or pathological evidence of heart failure in WKY ($n = 9$). Blood pressure and anatomical data are shown in Table 1. Blood pressure was higher and body weight lower in SHR. LV, right ventricle, and atria weight, in both absolute or body weight normalized values, were greater in SHR than WKY. Liver wet weight-to-dry weight, lung weight, and lung-to-body weight ratio were higher in SHR. Soleus weight was lower in SHR (WKY 0.157 ± 0.029; SHR 0.129 ± 0.021 g; $P = 0.044$).

3.2. Echocardiographic evaluation

Structural cardiac parameters are shown in Table 2. LV diastolic diameter (LVDD) and left atrium diameter-to-aortic diameter ratio were similar between groups. LVDD-to-body weight ratio, LV systolic diameter, LV diastolic posterior wall thickness, LV diastolic septal wall

Table 1
Blood pressure and anatomic data.

	WKY ($n=9$)	SHR ($n=8$)	P value
BP (mmHg)	118 ± 10	221 ± 35	<0.001
BW (g)	414 ± 57	295 ± 29	<0.001
LV weight (g)	0.80 ± 0.14	1.18 ± 0.24	<0.001
RV weight (g)	0.26 ± 0.04	0.50 ± 0.13	<0.001
Atria (g)	0.097 ± 0.018	0.243 ± 0.078	<0.001
LV weight/BW (mg/g)	1.94 ± 0.24	3.97 ± 0.49	<0.001
RV weight/BW (mg/g)	0.62 ± 0.08	1.70 ± 0.35	<0.001
Atria/BW (mg/g)	0.27 ± 0.05	0.82 ± 0.21	<0.001
Liver wet/dry	3.28 ± 0.07	3.53 ± 0.27	0.016
Lung (g)	2.32 ± 0.39	3.65 ± 1.0	0.002
Lung/BW (mg/g)	5.67 ± 1.13	12.39 ± 3.35	<0.001

WKY: normotensive rats; SHR: spontaneously hypertensive rats; n: number of animals; BP: systolic blood pressure; BW: body weight; LV: left ventricle; RV: right ventricle. Data are expressed as the mean ± standard deviation. Student's-t test.

Table 3
Left ventricular functional data.

	WKY ($n=9$)	SHR ($n=6$)	P value
HR (bpm)	253 ± 42	304 ± 21	0.016
FS (%)	54.6 ± 6.3	42.2 ± 7.1	0.003
EF	0.90 ± 0.04	0.80 ± 0.08	0.004
PWSV (mm/s)	32.9 ± 4.1	30.2 ± 4.9	0.256
E Wave (cm/s)	78.1 ± 14.1	71.7 ± 16.8	0.435
A Wave (cm/s)	45.0 ± 11.8	62.5 ± 25.4	0.091
E/A	1.83 ± 0.49	1.58 ± 1.48	0.639
ETD (ms)	44.3 ± 9.04	40.5 ± 14.9	0.646
IVRT (ms)	33.7 ± 4.18	38.0 ± 3.09	0.049

WKY: normotensive rats; SHR: spontaneously hypertensive rats; n: number of animals; HR: heart rate; FS: endocardial fractional shortening; EF: ejection fraction; PWSV: posterior wall shortening velocity; E/A: early-to-late diastolic mitral inflow ratio; EDT: E-wave deceleration time; IVRT: isovolumetric relaxation time. Data are expressed as the mean ± standard deviation. Student's-t test.

thickness, aorta diameter, left atrium diameter, and left atrium diameter-to-body weight ratio were higher in SHR than WKY.

Functional LV assessment results are shown in Table 3. Endocardial fractional shortening and LV ejection fraction were lower in SHR. Heart rate and isovolumic relaxation time were higher in SHR than WKY. Posterior wall shortening velocity, mitral A wave, mitral E wave, E/A ratio, and deceleration time of mitral E wave were not different between groups.

3.3. Morphologic study

Fiber cross sectional areas were lower (WKY 3.615 ± 412; SHR 2.035 ± 224 μm^2; P<0.001; Fig. 1), and collagen fractional area was higher (WKY 2.61 ± 0.39; SHR 4.88 ± 0.98%; P<0.001) in SHR.

3.4. Myosin heavy chain (MyHC) isoforms

The relative amount of the MyHC I isoform was higher in SHR than WKY (WKY 80.4 ± 3.33%; SHR 91.2 ± 3.33%; P = 0.003; Fig. 2).

3.5. Western blotting analysis

Myogenin protein levels were lower and MRF4 levels were higher in SHR (myogenin: WKY 1.00 ± 0.16; SHR 0.64 ± 0.35 arbitrary units; P = 0.02; MRF4: WKY 1.00 ± 0.27; SHR 1.53 ± 0.47 arbitrary units; P = 0.014; Fig. 3). MyoD was not statistically different between groups (WKY 1.00 ± 0.16; SHR 0.89 ± 0.22 arbitrary units; P = 0.29; Fig. 3). Myostatin and follistatin protein levels were lower in SHR (myostatin: WKY 1.00 ± 0.18; SHR 0.69 ± 0.24 arbitrary units; P = 0.01; follistatin: WKY 1.00 ± 0.17; SHR 0.65 ± 0.16 arbitrary units; P = 0.001; Fig. 4). The myostatin-to-follistatin expression ratio did not differ between groups (P > 0.05). Myogenin levels positively correlated with myocyte cross sectional area (r = 0.55; P = 0.033). MRF4 levels were positively correlated with relative amount of MyHC isoform I (r = 0.622; P = 0.013); there was a trend for MRF4 levels to negatively correlate with myocyte cross sectional area (r = −0.45; P = 0.08).

Table 2
Echocardiographic data.

	WKY ($n=9$)	SHR ($n=6$)	P value
LVDD (mm)	8.01 ± 0.95	8.64 ± 1.46	0.330
LVDD/BW (mm/kg)	19.6 ± 3.1	27.7 ± 4.7	0.001
LVSD (mm)	3.68 ± 0.92	5.08 ± 1.51	0.043
PWT (mm)	1.47 ± 0.06	1.82 ± 0.15	<0.001
SWT (mm)	1.49 ± 0.05	1.82 ± 0.15	<0.001
AO (mm)	4.49 ± 0.38	4.98 ± 0.34	0.024
LA (mm)	5.73 ± 0.59	7.28 ± 1.17	0.004
LA/AO	1.29 ± 0.19	1.47 ± 0.26	0.139
LA/BW (mm/kg)	13.9 ± 0.89	23.3 ± 3.43	<0.001

WKY: normotensive rats; SHR: spontaneously hypertensive rats; n: number of animals; LVDD and LVSD: left ventricle (LV) diastolic and systolic diameters, respectively; BW: body weight; PWT: LV diastolic posterior wall thickness; SWT: diastolic septal wall thickness; AO: aortic diameter; LA: left atrium diameter. Data are expressed as the mean ± standard deviation. Student's-t test.

4. Discussion

In this study, we showed that heart failure-induced skeletal myopathy in spontaneously hypertensive rats is characterized by atrophy, fibrosis, and changed myosin heavy chain isoforms. Phenotypical muscle alterations are combined with myogenic regulatory factors and myostatin and follistatin protein expression changes.

To the best of our knowledge, this is the first study to evaluate skeletal muscle in SHR with heart failure. The spontaneously hypertensive rat was introduced by Okamoto and Aoki as a genetic model of arterial hypertension [35]. Beginning at 18 months of age, rats develop heart failure features and evolve to death usually within

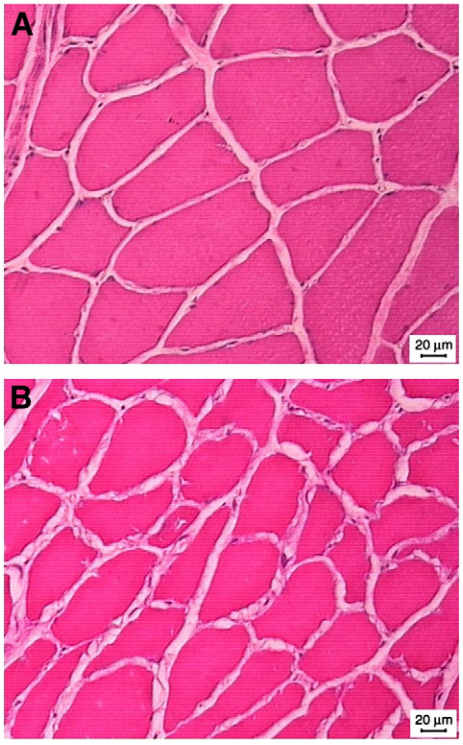

Fig. 1. Transverse histological sections of skeletal muscle soleus stained with hematoxylin-eosin. A: Wistar Kyoto rat; B: spontaneously hypertensive rat (SHR). Objetive: 40×.

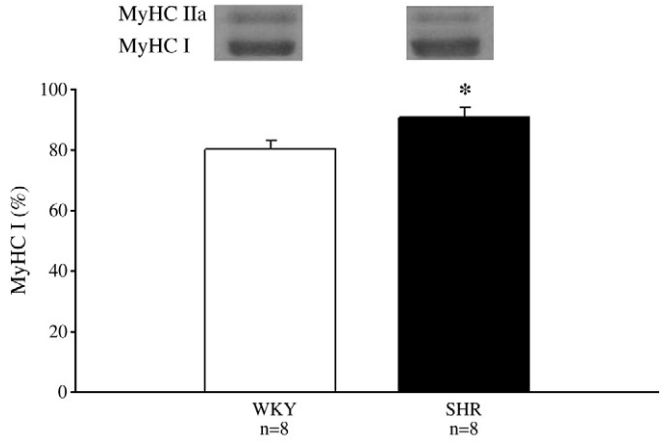

Fig. 2. Relative amount of myosin heavy chain (MyHC) I isoform of skeletal soleus muscle analysed by sodium dodecyl sulphate polyacrylamide gel electrophoresis. Data are expressed as mean ± standard deviation; * $P = 0.003$.

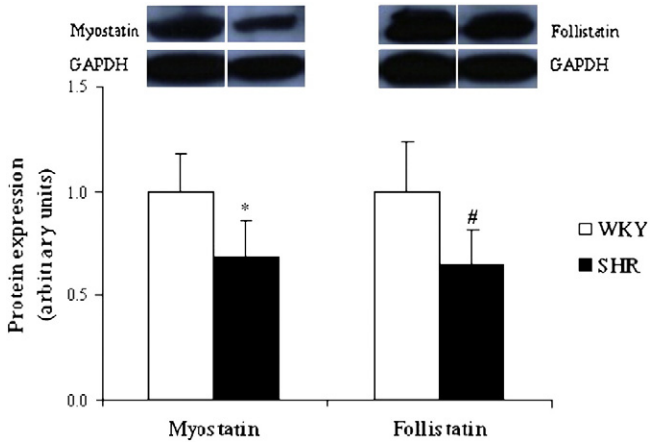

Fig. 4. Protein expression of myostatin and follistatin in soleus muscle analysed by Western blot ($n = 8$). Data expressed as mean ± standard deviation; * $P = 0.01$; # $P = 0.001$.

two to three weeks [26,27]. In this study, heart failure diagnosis was based on the presence of tachypnea and labored respiration and confirmed by pathological *post mortem* findings such as right ventricular hypertrophy, pleuropericardial effusion, pulmonary congestion, left atrial thrombus, and ascites. Systemic congestion was confirmed by the increased liver wet weight-to-dry weight ratio in the SHR group. Transthoracic echocardiography showed that SHR presented dilation of the left cardiac chambers, LV wall hypertrophy, and LV systolic dysfunction.

Skeletal muscle evaluation was performed in the soleus muscle, a muscle susceptible to acute and chronic heart failure conditions [7,36,37]. SHR presented significant muscle atrophy characterized by a 43.7% decrease in average muscle fiber cross sectional area compared to WKY. Decreased muscle fiber cross sectional area or diameter has been commonly observed in experimental heart failure, reducing between 9.7% and 16.5% from control values [6,7,16,38]. The significant degree of atrophy observed in SHR makes it particularly useful in studies for identifying the mechanisms and intracellular signaling pathways involved in heart failure-induced muscle atrophy.

Changes of skeletal MyHC isoform distribution have frequently been described during cardiac failure. In this study we found a relative increase of MyHC I isoform in SHR, suggesting a shift of muscle phenotype toward type I slow fibers, which have a predominantly oxidative metabolism [39]. During heart failure, other studies have reported both preserved MyHCs distribution [4,40] and increased MyHC II isoform [7,36,41,42], which contrast with our results. Six month-old SHRs have shown decreased MyHC I compared to age-matched WKY rats [43]. The variety of MyHC isoform distribution values seen during heart failure suggests that the molecular mechanisms involved in MyHC isoform modulation differ according to the heart failure model used [5,7,44].

We evaluated myogenic regulatory factors and myostatin/follistatin protein expression as potential mechanisms responsible for muscle atrophy and MyHC isoform changes. We observed decreased myogenin, myostatin, and follistatin; increased MRF4; and unchanged MyoD protein levels in the SHR group.

Myogenin is involved in satellite cells differentiation and myotube formation [13,45]. Decreased myogenin expression impairs fiber regeneration and may thus contribute to muscle atrophy [46]. In our study, decreased myogenin expression in SHR and a positive correlation between fiber cross-sectional area and myogenin levels suggest that this myogenic regulatory factor is involved in muscle atrophy. A similar result has been observed in the soleus muscle of rats with myocardial infarction-induced heart failure [5]. Myogenin is predominantly related to oxidative metabolism; one would therefore expect its reduced expression to have induced a decrease in type I MyHC isoform. However, we found increased type I MyHC isoform in SHR. As we evaluated the proportion of MyHCs isoforms in relation to total MyHC, we cannot rule out the possibility of a reduction in absolute amount of type I isoform. The mechanisms involved in myogenin reduction during heart failure are not completely understood. In cell culture, myogenin expression is

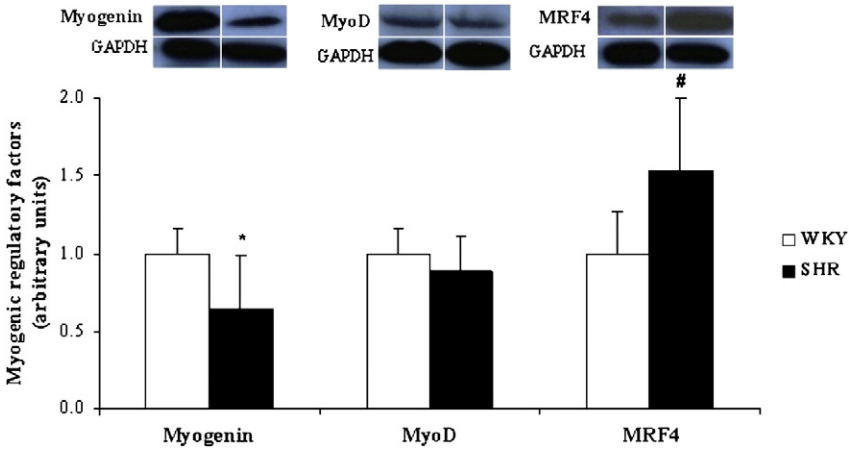

Fig. 3. Protein expression of myogenin, MyoD, and MRF4 in soleus muscle analysed by Western blot ($n = 8$). Data expressed as mean ± standard deviation; * $P = 0.02$; # $P = 0.014$.

supressed in differentiating myocytes treated with tumor necrosis factor-α, a cytokine which commonly increases during heart failure [46].

Myogenic regulatory factor MRF4 is predominantly expressed in slow oxidative fibers, and appears to play a role in modulating muscle phenotype. In this study, increased MRF4 protein expression in SHR was probably involved in the increased percentage of predominantly oxidative type I MyHC isoforms. Reinforcing this hypothesis, we observed a positive correlation between MRF4 protein expression and the relative amount of MyHC isoform I. The mechanisms responsible for changes in MRF4 expression are not clear. Myostatin-deficient double-muscled Japanese Shorthorn cattle exhibit increased MRF4 gene expression [47], suggesting that the decreased myostatin levels in our study may have played a role in increased MRF4 expression.

Increased myostatin expression has often been associated with reduced muscle mass in chronic diseases [48,49] and experimental muscle atrophy models [17,50]. Therefore, it was surprising to find decreased myostatin expression combined with significant muscle atrophy in our SHR group. Myostatin activity can be modulated by various proteins. One of the most studied myostatin antagonists is follistatin [21–23,51]. When administered to rats with portosystemic shunting, it resulted in increased muscle weight and lean body mass [52]. It has also been suggested that follistatin decreases skeletal muscle fibrosis and improves muscle healing after injury and disease [53,54]. Reduced follistatin levels in our study may have contributed to muscle fibrosis and atrophy despite reduced myostatin expression in the SHR group. Additionally, as follistatin can increase myogenin expression in cell culture preparations [53], its decreased levels could be involved in down-regulating myogenin in the SHR group. Few authors have investigated the myostatin pathway in cardiac failure [6,24]. Lenk et al. [24] observed that following experimental myocardial infarction, myostatin was up-regulated in gastrocnemius muscle, with values returning to baseline levels after exercise training. We previously observed that rats with long-term myocardial infarction-induced heart failure present muscle atrophy in combination with unchanged myostatin levels and decreased follistatin protein expression [6]. Additional studies are needed to better elucidate the relationship between myogenic regulatory factors, myostatin and the follistatin pathway, and muscle phenotype changes during heart failure.

In conclusion, heart failure-induced skeletal myopathy of spontaneously hypertensive rats is characterized by atrophy, fibrosis, and changed myosin heavy chain isoforms. Reduced myogenin and follistatin protein expression seems to participate in muscle atrophy while increased MRF4 protein expression can modulate myosin heavy chain isoform shift in the soleus muscle.

Acknowledgments

We are grateful to Jose Carlos Georgette and Vitor Marcos de Souza for their technical assistance and Colin Edward Knaggs for English editing. The authors of this manuscript certify that they complied with the Principles of Ethical Publishing in The International Journal of Cardiology.

References

[1] Mancini DM, Walter G, Reichek N, et al. Contribution of skeletal muscle atrophy to exercise intolerance and altered muscle metabolism in heart failure. Circulation 1992;85:1364–73.
[2] Strassburg S, Springer J, Anker SD. Muscle wasting in cardiac cachexia. Int J Biochem Cell Biol 2005;37:1938–47.
[3] Harrington D, Anker SD, Chua TP, et al. Skeletal muscle function and its relation to exercise tolerance in chronic heart failure. J Am Coll Cardiol 1997;30:1758–64.
[4] Anker SD, Sharma R. The syndrome of cardiac cachexia. Int J Cardiol 2002;85:51–66.
[5] Martinez PF, Okoshi K, Zornoff LAM, et al. Chronic heart failure-induced skeletal muscle atrophy, necrosis, and myogenic regulatory factors changes. Med Sci Monit 2010;16:374–83.
[6] Lima ARR, Martinez PF, Okoshi K, et al. Myostatin and follistatin expression in skeletal muscles of rats with chronic heart failure. Int J Exp Pathol 2010;91:54–62.
[7] Carvalho RF, Cicogna AC, Campos GER, et al. Myosin heavy chain expression and atrophy in rat skeletal muscle during transition from cardiac hypertrophy to heart failure. Int J Exp Pathol 2003;84:201–6.
[8] Sullivan MJ, Green HJ, Cobb FR. Skeletal muscle biochemistry and histology in ambulatory patients with long-term heart failure. Circulation 1990;81:518–27.
[9] Lipkin DP, Jones DA, Round JM, Poole-Wilson PA. Abnormalities of skeletal muscle in patients with chronic heart failure. Int J Cardiol 1988;8:187–95.
[10] Hughes SM, Koyshi K, Rudnicki M, Maggs AM. MyoD protein is differentially accumulated in fast and slow skeletal muscle fibres and required for normal fibre type balance in rodents. Mech Dev 1997;61:151–63.
[11] Megeney LA, Rudnicki MA. Determination versus differentiation and the MyoD family of transcription factors. Biochem Cell Biol 1995;73:723–32.
[12] Murre C, Mccaw PS, Vaessin H, et al. Interactions between heterologous helix-loop-helix proteins generate complexes that bind specifically to a common DNA sequence. Cell 1989;58:537–44.
[13] Hughes SM, Chi MM-Y, Lowry OH, Gundersen K. Myogenin induces a shift of enzyme activity from glycolytic to oxidative metabolism in muscles of transgenic mice. J Cell Biol 1999;145:633–42.
[14] Rudnicki MA, Schnegelsberg PNJ, Stead RH, Braun T, Arnold H-H, Jaenisch R. MyoD or Myf-5 is required for the formation of skeletal muscle. Cell 1993;75:1351–9.
[15] Loughna PT, Brownson C. Two myogenic regulatory factor transcripts exhibit muscle-specific responses to disuse and passive stretch in adult rats. FEBS Lett 1996;390:304–6.
[16] Carvalho RF, Cicogna AC, Campos GER, et al. Heart failure alters MyoD and MRF4 expressions in rat skeletal muscle. Int J Exp Pathol 2006;87:219–25.
[17] Lee SJ. Regulation of muscle mass by myostatin. Annu Rev Cell Dev Biol 2004;20:61–86.
[18] McPherron AC, Lawler AM, Lee S-J. Regulation of skeletal muscle mass in mice by a new TGF-beta superfamily member. Nature 1997;387:83–90.
[19] Carlson CJ, Booth FW, Gordon SE. Skeletal muscle myostatin mRNA expression is fiber-type specific and increases during hindlimb unloading. Am J Physiol 1999;277:R601–6.
[20] Reardon KA, Davis J, Kapsa RM, Choong P, Byrne E. Myostatin, insulin-like growth factor-1, and leukemia inhibitory factor mRNAs are upregulated in chronic human disuse muscle atrophy. Muscle Nerve 2001;24:893–9.
[21] Lee S-J, McPherron AC. Regulation of myostatin activity and muscle growth. Proc Natl Acad Sci U S A 2001;98:9306–11.
[22] Amthor H, Nicholas G, McKinnell I, et al. Follistatin complexes myostatin and antagonises myostatin-mediated inhibition of myogenesis. Dev Biol 2004;270:19–30.
[23] Nakatani M, Takehara Y, Sugino H, et al. Transgenic expression of a myostatin inhibitor derived from follistatin increases skeletal muscle mass and ameliorates dystrophic pathology in mdx mice. FASEB J 2008;22:477–87.
[24] Lenk K, Schur R, Linke A, et al. Impact of exercise training on myostatin expression in the myocardium and skeletal muscle in a chronic heart failure model. Eur J Heart Fail 2009;11:342–8.
[25] Woodiwiss AJ, Tsotetsi OJ, Sprott S, et al. Reduction in myocardial collagen cross-linking parallels left ventricular dilatation in rats models of systolic chamber dysfunction. Circulation 2001;103:155–60.
[26] Bing OHL, Brooks WW, Robinson KG, et al. The spontaneously hypertensive rat as a model of the transition from compensated left ventricular hypertrophy to failure. J Mol Cell Cardiol 1995;27:383–96.
[27] Cicogna AC, Robinson KG, Conrad CH, et al. Direct effects of colchicine on myocardial function. Studies in hypertrophied and failing spontaneously hypertensive rats. Hypertension 1999;33:60–5.
[28] Conrad CH, Brooks WW, Robinson KG, Bing OHL. Impaired myocardial function in spontaneously hypertensive rats with heart failure. Am J Physiol 1991;260:H136–45.
[29] Martinez PF, Okoshi K, Zornoff LAM, et al. Echocardiographic detection of congestive heart failure in postinfarction rats. J Appl Physiol 2011;111:543–51.
[30] Paiva SAR, Zornoff LAM, Okoshi MP, et al. Ventricular remodeling induced by retinoic acid supplementation in adult rats. Am J Physiol Heart Circ Physiol 2003;284:H2242–6.
[31] Lang RM, Bierig M, Devereux RB, et al. Recommendations for chamber quantification: a report from the American Society of Echocardiography's Guidelines and Standards Committee and the Chamber Quantification Writing Group, developed in conjunction with the European Association of Echocardiography, a branch of the European Society of Cardiology. J Am Soc Echocardiogr 2005;18:1440–63.
[32] Okoshi MP, Matsubara LS, Franco M, Cicogna AC, Matsubara BB. Myocyte necrosis is the basis for fibrosis in renovascular hypertensive rats. Braz J Med Biol Res 1997;30:1135–44.
[33] Okoshi K, Nakayama M, Yan X, et al. Neuregulins regulate cardiac parasympathetic activity. Muscarinic modulation of beta-adrenergic activity in myocytes from mice with neuregulin-1 gene deletion. Circulation 2004;110:713–7.
[34] Dasarathy S, Muc S, Hisamuddin K, et al. Altered expression of genes regulating skeletal muscle mass in the portcaval anastomosis rat. Am J Physiol Gastrointest Liver Physiol 2007;292:G1105–13.
[35] Okamoto K, Aoki K. Development of a strain of spontaneously hypertensive rats. Jpn Circ J 1963;27:282–93.
[36] De Sousa E, Veksler V, Bigard X, Mateo P, Ventura-Clapier R. Heart failure affects mitochondrial but not myofibrillar intrinsic properties of skeletal muscle. Circulation 2000;102:1847–53.

[37] Carvalho RF, Dariolli R, Justulin Junior LA, et al. Heart failure alters matrix metalloproteinase gene expression and activity in rat skeletal muscle. Int J Exp Pathol 2006;87:437–43.
[38] Santos DP, Okoshi K, Moreira VO, et al. Growth hormone attenuates skeletal muscle changes in experimental chronic heart failure. Growth Horm IGF Res 2010;20:149–55.
[39] Simonini A, Massie BM, Long CS, Qi M, Samarel AM. Alterations in skeletal muscle gene expression in the rat with chronic congestive heart failure. J Mol Cell Cardiol 1996;28:1683–91.
[40] Coirault C, Guellich A, Barbry T, Samuel JL, Riou B, Lecarpentier Y. Oxidative stress of myosin contributes to skeletal muscle dysfunction in rats with chronic heart failure. Am J Physiol Heart Circ Physiol 2007;292:H1009–17.
[41] Vescovo G, Ceconi C, Bernocchi P, et al. Skeletal muscle myosin heavy chain expression in rats with monocrotaline-induced cardiac hypertrophy and failure. Relation to blood flow and degree of muscle atrophy. Cardiovasc Res 1998;39: 233–41.
[42] Dalla Libera L, Zennaro R, Sandri M, Ambrosio GB, Vescovo G. Apoptosis and atrophy in rat slow skeletal muscles in chronic heart failure. Am J Physiol Cell Physiol 1999;277:C982–6.
[43] Bortolotto SK, Stephenson DG, Stephenson GMM. Fiber type populations and Ca^{2+}-activation properties of single fibers in soleus muscles from SHR and WKY rats. Am J Physiol Cell Physiol 1999;276:C628–37.
[44] Spangenburg EE, Talmadge RJ, Musch TI, Pfeifer PC, McAllister RM, Williams JH. Changes in skeletal muscle myosin heavy chain isoform content during congestive heart failure. Eur J Appl Physiol 2002;87:182–6.
[45] Ekmark M, Gronevik E, Schjerling P, Gundersen K. Myogenin induces higher oxidative capacity in pre-existing mouse muscle fibres after somatic DNA transfer. J Physiol 2003;548:259–69.
[46] Langen RCJ, Schols AMWJ, Kelders MCJM, Wouters EFM, Janssen-Heininger YMW. Inflammatory cytokines inhibit myogenic differentiation through activation of nuclear factor-kappaB. FASEB J 2001;15:1169–80.
[47] Muroya S, Watanabe K, Hayashi S, et al. Muscle type-specific effect of myostatin deficiency on myogenic regulatory factor expression in adult double-muscled Japanese Shorthorn cattle. Anim Sci J 2009;80:678–85.
[48] Bruera E, Sweeney C. Cachexia and asthenia in cancer patients. Lancet Oncol 2000;1:138–47.
[49] Gonzalez-Cadavid NF, Taylor WE, Yarasheski K, et al. Organization of the human myostatin gene and expression in healthy men and HIV-infected men with muscle wasting. Proc Natl Acad Sci U S A 1998;95:14938–43.
[50] Baumann AP, Ibebunjo C, Grasser WA, Paralkar VM. Myostatin expression in age and denervation-induced skeletal muscle atrophy. J Musculoskelet Neuronal Interact 2003;3:8–16.
[51] Rodino-Klapac LR, Haidet AM, Kota C, Handy C, Kaspar BK, Mendell JR. Inhibition of myostatin with emphasis on follistatin as a therapy for muscle disease. Muscle Nerve 2009;39:283–96.
[52] Dasarathy S, McCullough AJ, Muc S, et al. Sarcopenia associated with portosystemic shunting is reversed by follistatin. J Hepatol 2011;54:915–21.
[53] Zhu J, Li Y, Lu A, et al. Follistatin improves skeletal muscle healing after injury and disease through an interaction with muscle regeneration, angiogenesis, and fibrosis. Am J Pathol 2011;179:915–30.
[54] Lee SJ, Lee YS, Zimmers TA, et al. Regulation of muscle mass by follistatin and activins. Mol Endocrinol 2010;24:1998–2008.